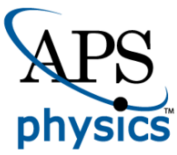

Electron-phonon coupling mechanisms for hydrogen-rich metals at high pressure

K. Tanaka, J. S. Tse, and H. Liu

Phys. Rev. B **96**, 100502 — Published 11 September 2017

DOI: 10.1103/PhysRevB.96.100502

Electron-phonon coupling mechanisms for hydrogen-rich metals at high pressure

K. Tanaka,[1,*] J. S. Tse,[1,2,†] and H. Liu[1,3]

[1] *Department of Physics and Engineering Physics, University of Saskatchewan, 116 Science Place, Saskatoon, SK, S7N 5E2 Canada*
[2] *State Key Laboratory for Superhard Materials, Jilin University, Changchun 130012, China*
[3] *Geophysical Laboratory, Carnegie Institution for Science, Washington, DC 20015, USA*

(Dated: August 28, 2017)

The mechanisms for strong electron-phonon coupling predicted for hydrogen-rich alloys with high superconducting critical temperature (T_c) are examined within the Migdal-Eliashberg theory. Analysis of the functional derivative of T_c with respect to the electron-phonon spectral function shows that at low pressures, when the alloys often adopt layered structures, bending vibrations have the most dominant effect. At very high pressures, the H-H interactions in two-dimensional (2D) and three-dimensional (3D) extended structures are weakened, resulting in mixed bent (libration) and stretch vibrations, and the electron-phonon coupling process is distributed over a broad frequency range leading to very high T_c.

PACS numbers: 74.20.Pq, 74.25.Kc, 74.62.Bf, 74.62.Fj,

Hydrogen is the lightest element and thus, if molecular hydrogen can be compressed into a metal in the solid state, it is expected to become superconducting at a very high transition temperature T_c due to exceptionally strong electron-phonon coupling[1]. Although this proposal has not been verified experimentally, calculation based on modern electronic structure theory has predicted high T_c for metallic hydrogen[2,3]. According to recent studies, metallization of solid hydrogen may require pressure in excess of 400 GPa, which is difficult to achieve with today's experimental techniques. Although very recently metallic hydrogen has been claimed to be observed under extremely high pressure of nominal 495 GPa[4], the result is contentious[5] and further experiments are required. On the other hand, it has been realised that the electron density required to metallize molecular hydrogen may be achieved by compression of group-IVa hydrides, in which the hydrogen content is already high[6]. This insightful suggestion has stimulated various theoretical studies and experimental investigations. The first prediction of superconductivity in group-IVa hydrides was made using density functional theory for silane (SiH_4)[7]. First-principles calculation has predicted a monoclinic $C2/c$ metallic solid composed of SiH_4 layers bridged by Si-H-Si bonds that is stable between 65 and 150 GPa and has T_c of 45-55 K at 90-125 GPa[8]. Subsequent experiment has revealed that insulating molecular silane transforms to a metal at 50 GPa and becomes superconducting with $T_c = 17$ K at 96 and 120 GPa[9]. However, the measured diffraction pattern of the superconducting phase did not match the monoclinic structure[9] and the high-pressure structure of silane remains controversial[10].

In the past decade, numerous theoretical predictions have been made on the structure and superconducting behaviour of stoichiometric and hydrogen-enriched hydrides with a variety of elements at high pressures. Most notable examples are the high-pressure polymorphs of CaH_6 and YH_6, both of which have a novel cagelike structure formed by monatomic hydrogens and have been predicted to have T_c higher than 200 K[11,12]. A major experimental breakthrough has been reported recently with the observation of superconductivity with a critical temperature above 200 K in hydrogen sulfide (H_2S) compressed to $\sim$ 200 GPa[13]. Isotopic, magnetic and Meissner-effect measurements have shown that superconductivity is driven by electron-phonon interactions. Electronic structure and electron-phonon coupling calculations[14–16] and x-ray diffraction experiment[17] have determined that the superconducting phase consists of the decomposed product H_3S with a cubic structure. The surprisingly high observed T_c raises the possibility that even higher transition temperatures may be attainable in hydrides. So far, the predictions of superconductivity and T_c in hydrides have entirely relied on calculation for selected structures. It is desirable that general rules can be established to understand the underlying mechanisms of high-T_c superconductivity in hydrogen-rich materials.

In this work, by solving the Eliashberg equations[18–20], we analyse the functional derivative of T_c with respect to the electron-phonon spectral function $\alpha^2F(\omega)$ of several representative hydride systems to characterise the most effective vibrational modes for enhancement of superconductivity. Our goal is to develop a strategy for synthesising new compounds with high critical temperatures. The functional derivative $\delta T_c/\delta\alpha^2F(\omega)$[21] enables us to identify the frequency regions where phonons are most effective in raising T_c[22–24]. We evaluate the functional derivative from the electron-phonon spectral functions calculated from linear response theory and density functional perturbation theory, either performed for the present study or taken from reports of previous theoretical studies.

A survey of theoretically predicted hydrogen-dominant main group metallic alloys under high pressures reveals that most alloys adopt a layered structure. For this group of compounds, the calculated $T_c < 100$ K. We have chosen to examine SnH_4 in detail as the superconducting metallic phase that is stable between 70 to 160 GPa and

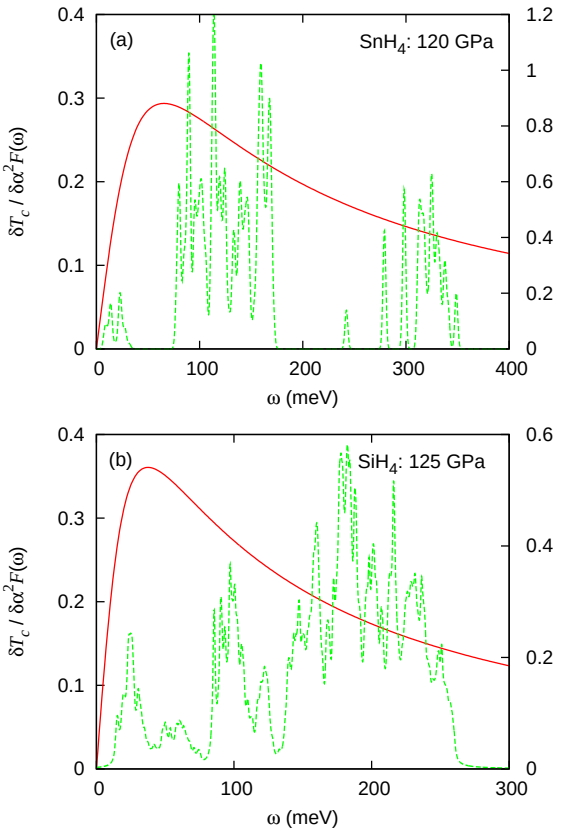

FIG. 1. (Colour online) The functional derivative $\delta T_c/\delta\alpha^2F(\omega)$ (red solid curve) and the electron-phonon spectral function $\alpha^2F(\omega)$ (green dashed curve) as a function of frequency ω for (a) SnH_4 at 120 GPa and (b) SiH_4 at 125 GPa.

has a novel layered structure intercalated by "H_2" units with high T_c[25]. A remarkable feature of this structure is that the phonon band structure and the spectral function can be separated into three distinct frequency regions, corresponding to lattice (L), Sn-H, and H_2 vibrations with increasing frequency, as can be seen in Fig. 1(a). This unique property facilitates the analysis of the contributions of different vibrational bands to superconductivity, as the spectral function $\alpha^2F(\omega)$ can be decomposed as $\alpha^2F(\omega)_{\rm L} + \alpha^2F(\omega)_{\rm Sn\text{-}H} + \alpha^2F(\omega)_{\rm H\text{-}H}$. The electron-phonon coupling (EPC) parameter λ is twice the first inverse moment of the spectral function, $\lambda = 2\int d\omega\, \frac{\alpha^2F(\omega)}{\omega}$. The EPC parameter $\lambda(\omega)$ integrated up to frequency ω of SnH_4 has shown that the lattice and Sn-H librations contribute most to the process of electron-phonon coupling, while there is only very minor contribution from the H-H vibrations[25]. We have calculated T_c from the individual vibrational bands by solving the Eliashberg equations at 120 GPa, using the Coulomb pseudopotential $\mu^*(\omega_{\rm max})$ scaled to $\omega_{\rm max}$, where $\omega_{\rm max}$ is six times the maximum phonon frequency. For $\mu^*(\omega_{\rm max}) = 0.1$, the entire spectrum yields $T_c \simeq 98$ K. Removing the low-frequency lattice vibrations from the spectrum only reduces T_c roughly by 4 K, while eliminating the high-frequency H-H contribution results in $T_c \simeq 72$ K. In fact, the Sn-H vibrational band by itself yields $T_c \simeq 66$ K. Thus, the Sn-H vibrations are the most dominant contribution to T_c. The functional derivative shown in Fig. 1(a) is maximum at about 65 meV. This optimal frequency, $\omega_{\rm opt}$, is close to the onset of the Sn-H bending vibrations. Therefore, it is plausible that variation of the bending vibrations can affect the critical temperature significantly. The optimal frequency is known to be related to the critical temperature by $\omega_{\rm opt} \sim 7k_BT_c$[19,26], where k_B is the Boltzmann constant. Using this relation, T_c is estimated to be roughly 108 K, in good agreement with 98 K from solving the Eliashberg equations.

The functional derivative for the monoclinic SiH_4 structure at 125 GPa is presented in Fig. 1(b). For this compound, no H-H species are present and partition of the phonon spectrum to lattice, Si-H bent (libration) and stretch vibrations is less distinctive. For $\mu^*(\omega_{\rm max}) = 0.1$, the optimal vibrational frequency is found to be 38 meV, in the frequency range between the lattice and low-frequency Si-H bending vibrations. T_c estimated from $\omega_{\rm opt} \sim 7k_BT_c$ is about 63 K, again comparable to 53 K obtained from the Eliashberg equations. The above results on SnH_4 and SiH_4 highlight the importance of lattice and bending vibrations on the electron-phonon coupling process. It is surprising, however, that the low-frequency lattice vibrations in SnH_4 contribute substantially to the EPC parameter[25], but not so much to T_c. This implies that a higher critical temperature cannot necessarily be achieved by simply increasing the mass of the heavier element in hydrides.

Study of a series of high-pressure yttrium hydrides (YH_n, $n = 3$, 4 and 6) offers useful insight into the evolution of crystal structure and the superconducting properties as the hydrogen concentration is increased beyond what is required to satisfy the normal covalency (i.e., YH_3). YH_3 has been predicted to have a face-centered cubic structure formed from monoatomic H situated in the tetrahedral and octahedral interstitial sites and separated by long distances[12]. This structure is stable from 17.7 GPa to 140 GPa. Similarly to SnH_4, the spectral function can clearly be separated into regions for lattice, Y-H and H-H vibrations. At 17.7 GPa, the H-H vibration energy of 165 meV is much lower than that of normal H_2 at the same pressure. The compound is predicted to be superconducting with maximum T_c of 40 K at 17.7 GPa. Upon compression, T_c decreases and superconductivity vanishes between 35 and 44 GPa, only to reappear at a lower value of around 6 K at higher pressure. Two energetically competing hydrogen-rich polymorphs YH_4 (YH_3+H_2) and YH_6 ($2YH_3 + 3H_2$) have been predicted to be thermodynamically more stable than the product of YH_3 and solid H_2 above 140 GPa. Both are superconductors with maximum T_c of 85 K and 235 K for YH_4

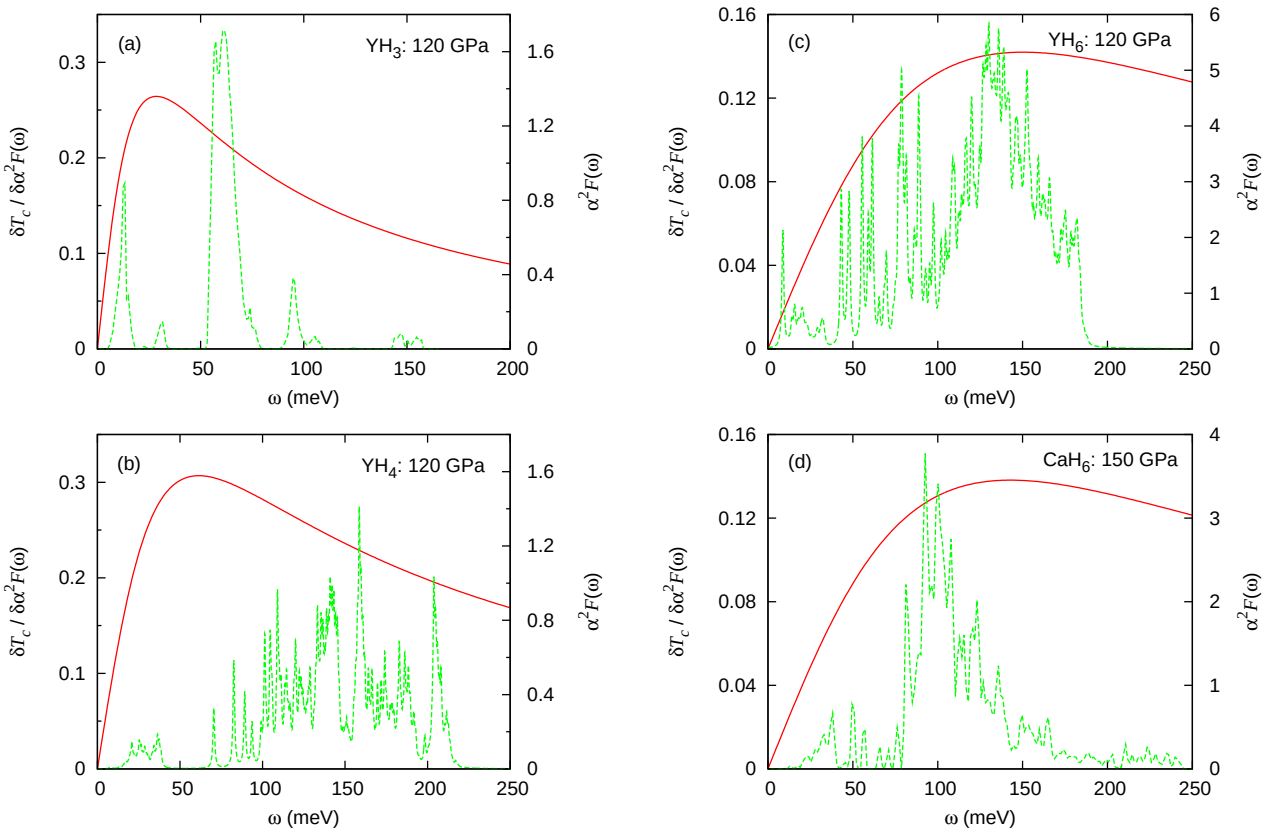

FIG. 2. (Colour online) The functional derivative $\delta T_c/\delta\alpha^2F(\omega)$ (red solid curve) and the electron-phonon spectral function $\alpha^2F(\omega)$ (green dashed curve) as a function of frequency ω for (a) YH_3, (b) YH_4 and (c) YH_6 at 120 GPa, and (d) CaH_6 at 150 GPa.

and YH_6, respectively. As mentioned above, YH_3 has a cubic structure composed of atomic hydrogens. YH_4 has tetragonal space group and consists of atomic H and molecular "H_2". YH_6 has a novel cubic cage structure with Y located in the sodalite cages formed by H atoms. The same structure has also been found in CaH_6 which too is predicted to be a good superconductor with T_c of 205 K at 150 GPa[11]. Changes in the H network topology in these structures can be rationalised by a charge transfer model proposed earlier for Ca and Sr hydrides[11,27]. Y is trivalent with a valence shell electron configuration $4d^15s^2$. Since $4d$ and $5s$ orbitals are shielded by their respective core orbitals, the valence electrons can be removed easily. Assuming full charge transfer as expected in YH_3, the effective electron number (EEN) of each hydrogen is $-1e$ and thus leads to the formation of monatomic hydrogens in the crystal structure. On the other hand, in YH_4, the EEN is $(3/4)e$ and hence some of the "molecular H_2" are preserved, albeit with a long H-H bond length of 1.33 Å at 120 GPa. In YH_6, the EEN is further reduced to $(1/2)e$, but to maintain maximum overlaps of the H orbitals, the cage structure is preferred. The features of H-H interactions in these crystal structures suggest the existence of high-frequency H-H vibrons in YH_4, YH_6, and YH_3 with frequency in descending order. This trend has indeed been confirmed by phonon band structure calculations[12]. The predicted maximum T_c, however, does not follow this sequence. Therefore, the mean vibrational frequency, $\langle\omega\rangle$, often used in estimating the critical temperature in terms of the McMillan[28] or Allen-Dynes[29,30] equation, is not necessarily the only factor to be considered for raising T_c.

To gain insight into the role of phonons in the superconducting state, the functional derivative $\delta T_c/\delta\alpha^2F(\omega)$ has been computed for YH_3, YH_4, and YH_6 for $\mu^*(\omega_{\rm max}) = 0.1$ and the results are compared in Fig. 2. The respective optimal frequencies are 29, 61 and 150 meV with $T_c \sim \omega_{\rm opt}/7k_B$ of 48, 101 and 249 K, respectively, which compare well with T_c of 43, 92 and 247 K calculated from the Eliashberg equations. An interesting aspect of the optimal vibrations is that in YH_3 it is maximised at the lattice acoustic translational branch, while

in YH_4, it originates from the soft vibrational branch of the localised "molecular H_2" units. In YH_6, there is no clear distinction between stretch and bent modes as the H atoms form a 3D connected open sodalite framework. Coupling of these vibrations results in the continuous spectral distribution. These vibrations all participate strongly in the electron-phonon interaction and shift the optimal frequency to higher energy, yielding a higher T_c. Moreover, the functional derivative curve is broad and does not taper off as rapidly at higher frequency as in YH_3 and YH_4. For comparison, the functional derivative of the isostructural CaH_6 is also examined [Fig. 2(d)]. Once again a continuous distribution of H-dominated vibrations is observed. In this case, the maximum of the functional derivative is located at 143 meV. Although the functional derivative profiles for YH_6 and CaH_6 are broadly similar, it is important to note that the H-H distance in YH_6 of 1.31 Å is significantly larger than 1.24 Å in CaH_6 under similar pressure. A larger H-H distance in YH_6 can be understood as due to the fact that there is one more valence electron provided by Y than by Ca (three vs. two). Thus, the EEN of the H atom is higher in YH_6, leading to a weaker and longer "molecular H_2" bond. The cutoff frequency for the H-H vibrons in CaH_6 (245 meV) is therefore higher than in YH_6 ($\sim$ 189 meV), but the optimal frequency is lower.

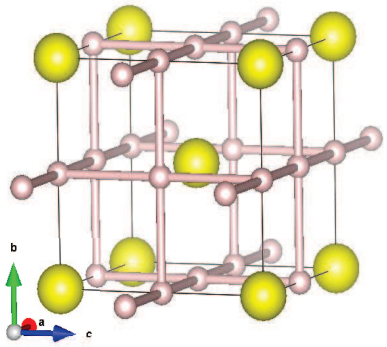

FIG. 3. (Colour online) Crystal structure of H_3S.

The above observation clearly shows that the signature of a high-T_c hydrogen-rich material is the presence of strongly coupled hydrogen-dominant libration and stretch vibrations. As demonstrated above, weak H-H interactions with bond length of 1.2-1.3 Å is desirable. At this bond separation, there is no longer clear distinction between stretch and bent vibrations and all H vibrations participate effectively in the electron-phonon coupling process. Another example is the recently discovered high critical temperature in compressed H_2S at $\sim$ 200 GPa[13]. The functional derivative of the spectral function of the candidate H_3S has been analysed[24] and the major feature in the spectral function is again found to be the hydrogen libration and stretch vibrations being strongly mixed. However, an important point is that the body centered cubic structure may be viewed as the sulfur atoms being enclathrated at the center of a cubic box created by a 3D hydrogen network (Fig. 3). Therefore, based on the proposed charge transfer model[11,27], the design of materials possessing this unique structural property requires consideration of both the hydrogen concentration and the nature and number of available valence electrons from the donor atom. For example, the sodalite structure is severely distorted when Ca is replaced by the similarly divalent Sr in SrH_6, as Sr can no longer be accommodated in the cage due to the large atomic size.

Our findings are consistent with a very recent study of La-H and Y-H systems in terms of density functional theory, where LaH_{10} and YH_{10} have been found to adopt a sodalite-like face-centered cubic structure and have T_c in the range of room temperature[32]. We have also solved the Eliashberg equations for these systems and have found that $\delta T_c/\delta\alpha^2F(\omega)$ has a broad distribution and decays rather slowly beyond $\omega_{\rm opt}$, similarly to that for YH_6 and CaH_6 shown in Fig. 2(c) and (d). In Table I we summarise key quantities for superconductivity for the systems studied in this work, including YH_{10} and LaH_{10}[33]. It can be seen that $\omega_{\rm opt}$ and hence T_c are the highest for YH_{10} at 250 GPa, even though λ is smaller compared to YH_6 or SrH_{10} (see below).

The sodalite cage structure is not the only structural motif that can support high electron-phonon coupling. Dense molecular hydrogen with the orthorhombic structure (*Cmca*) has been predicted from superconductivity density functional theory to have a critical temperature of 242K at 450 GPa[31]. The crystal structure at 300 GPa shown in Fig. 4(a) is composed of staggered 2D puckered honeycomb layers with interatomic distances alternating between 0.78 and 1.10 Å. The closest H-H distance between two layers is 1.27 Å. The calculated electron-phonon spectral function is almost continuous up to 494 meV with lattice, libration and molecular vibrations all strongly coupled to the electrons. One may ask, is it possible to construct a similar structural morphology in hydrogen-rich alloys? In a survey of hydrogen-rich strontium hydrides, a high-pressure polymorph, SrH_{10}, a rhombohedral crystal with planes of Sr sandwiched between every two puckered honeycomb H layers and H-H bonds alternating between 0.998 and 1.011 Å has been found to be stable above 300 GPa [Fig. 4(b)]. The similarity in the structure to the *Cmca* metallic phase of solid hydrogen is striking and suggests potential superconductivity with a high transition temperature. To examine this possibility, the electronic and phonon band structure and electron-phonon coupling for the 300 GPa structure have been calculated using density functional theory. The phonon band structure presented in Fig. 4(c) exhibits strong electron-phonon couplings from the librational phonon branches between 50 and 160 meV along the $X \rightarrow \Gamma \rightarrow T$ symmetry direction. SrH_{10} is indeed a superconductor and the calculated isotropic EPC parameter λ is 3.08 and the T_c calculated from the Eliashberg equations is 259 K with $\mu^*(\omega_{\rm max}) = 0.1$. The functional derivative is presented in Fig. 4(d). As in metallic hy-

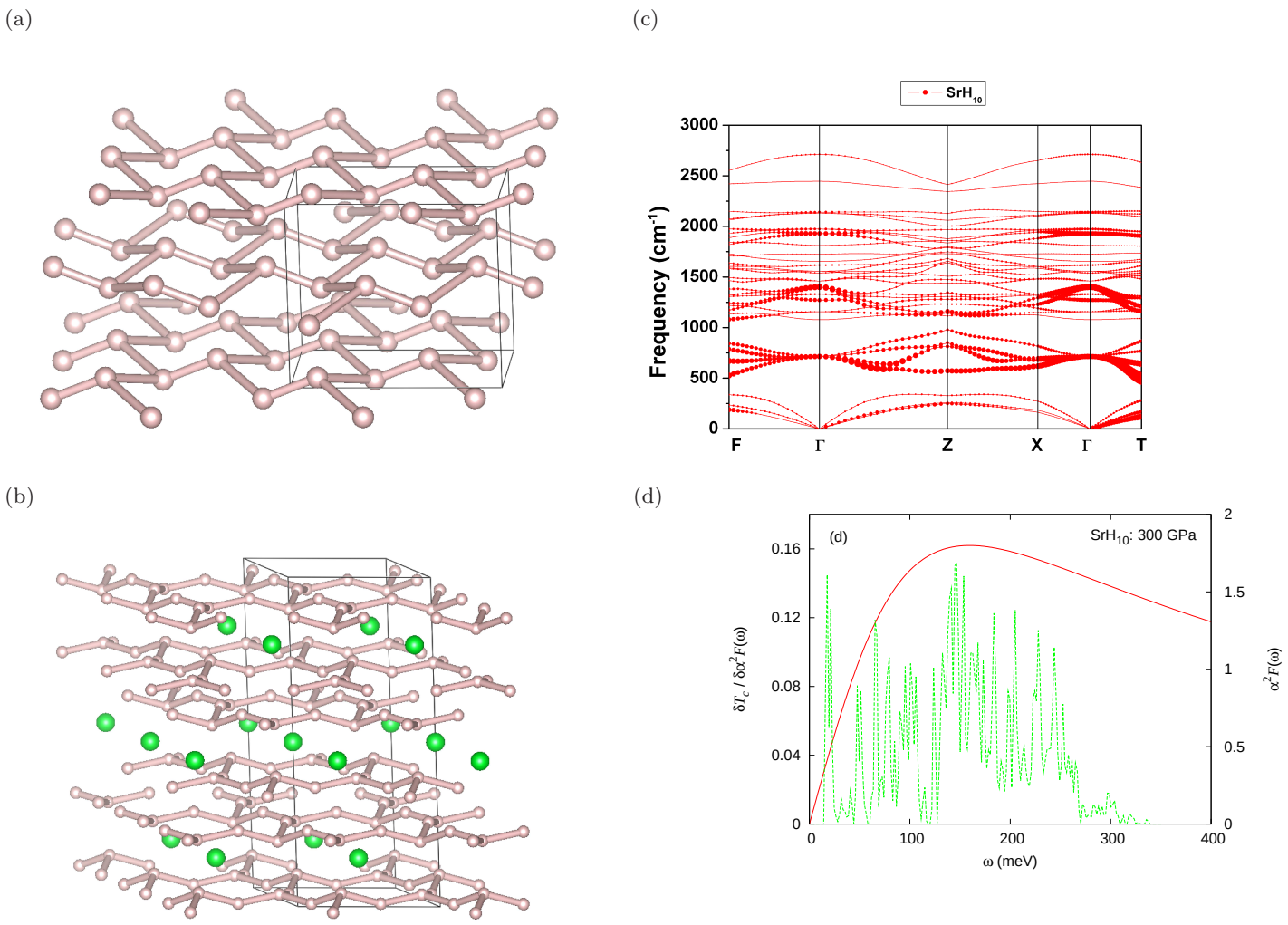

FIG. 4. (Colour online) (a) *Cmca* structure of molecular hydrogen at 300 GPa, (b) rhombohedral crystal structure of SrH_{10}, (c) phonon band structure of SrH_{10} at 300 GPa, and (d) $\delta T_c/\delta\alpha^2F(\omega)$ (red solid curve) and $\alpha^2F(\omega)$ (green dashed curve) as a function of frequency ω for SrH_{10} at 300 GPa.

drogen, the distribution of the phonon modes is almost continuous with the functional derivative maximised at 159 meV. In this case, the high-frequency H-H stretch vibrations centered around 270 meV contribute very little to the overall coupling with electrons. These results confirm the expectation and show, as the sodalite structure, the unique layer H-network morphology is relevant to high-temperature superconductivity. So far, the sodalite and puckered honeycomb layer H-networks are the only two structural features found in hydrogen-rich materials possessing very high T_c ($>$ 200 K) by theoretical calculations.

In summary, we have shown from analysis of the structures and functional derivative of selected high-pressure hydrides that the metallic-H bent (or librational) vibrations are most effective in enhancing the superconducting transition temperature. Furthermore, since the vibration profile (or the electron-phonon spectral function) is intimately related to the crystal structure, two types of H networks, the sodalite and puckered honeycomb layer structures with strong mixing of stretch and bent vibrations are most likely to lead to strong electron-phonon coupling for all the modes. Can room-temperature superconductivity be achieved if the phonon-mediated Eliashberg theory is valid? From the relation $\omega_{\rm opt} \sim 7k_BT_c$, the optimal frequency should be 180 meV (1450 cm^{-1}) for a critical temperature $T_c = 300$ K. Among the results presented in Table I, YH_{10} at 250 GPa is close to ideal. The key is to prepare a system with a broad vibration distribution and efficient electron-phonon coupling close to this frequency. As illustrated above, the functional derivative of the sodalite structures (CaH_6 and YH_6) does not decrease as quickly above the optimal frequency as the other structures, indicating that all the modes, with the

TABLE I. T_c obtained by solving the Eliashberg equations, the EPC parameter λ, the optimal frequency $\omega_{\rm opt}$, the average phonon frequency $\langle\omega\rangle$, $\omega_{\rm log}$ in the Allen-Dynes-modified McMillan equation[30], and the H-H distance in the H network for various systems studied. In SiH_4 hydrogens do not form a network by themselves. $\mu^*(\omega_{\rm max}) = 0.1$ has been used throughout.

System	Pressure (GPa)	T_c (K)	λ	$\omega_{\rm opt}$ (meV)	$\omega_{\rm opt}/7k_B$ (K)	$\langle\omega\rangle$ (meV)	$\omega_{\rm log}$ (meV)	H-H distance (Å)
SiH_4	125	53	0.89	38	63	111	79	–
SnH_4	120	98	1.20	65	108	111	76	0.841
YH_6	120	247	3.19	150	249	87	63	1.306
YH_{10}	250	291	2.67	177	293	97	95	1.132
YH_{10}	300	275	2.00	170	282	147	125	1.029
LaH_{10}	300	231	1.74	144	239	142	123	1.076
CaH_6	150	235	2.71	143	237	96	87	1.238
SrH_{10}	300	259	3.08	159	264	96	66	0.997

exception of lattice vibrations, are very efficient in enhancing T_c. Moreover, the spectral function shows that the electron-phonon coupling strength (the area under the spectrum) is uniformly large for these structures. In principle, it is plausible to design materials with such characteristics, perhaps by choosing a di- or trivalent element with a valence electron ionization energy (electron donating property) intermediate between Ca and Y such that the H-H distance in the sodalite structure is about halfway ($\simeq 1.27$Å). This will decrease the stretch frequency but maintain strong electron-phonon coupling. Another possibility is to increase the H_2 concentration in compounds with electron donating atoms. As observed in SrH_{10} above, the metallic atoms help to reduce the pressure required to form the puckered "molecular" H_2 layers in superconducting solid hydrogen.

The research was supported by the Natural Sciences and Engineering Research Council of Canada and the Canada Foundation for Innovation.

* kat221@campus.usask.ca
† john.tse@usask.ca

[1] N. W. Ashcroft, Phys. Rev. Lett. **21**, 1748 (1968).
[2] P. Cudazzo, G. Profeta, A. Sanna, A. Floris, A. Continenza, S. Massidda, and E. K. U. Gross, Phys. Rev. B **81**, 134506 (2010).
[3] J. M. McMahon and D. M. Ceperley, Phys. Rev. B **84**, 144515 (2011); *ibid.* **85**, 219902(E) (2012).
[4] R. P. Dias and I. F. Silvera, Science **355**, 715 (2017).
[5] D. Castelvecchi, Nature **542**, 17 (2017); R. F. Service, Science **355**, 332 (2017).
[6] N. W. Ashcroft, Phys. Rev. Lett. **92**, 187002 (2004).
[7] J. Feng, W. Grochala, T. Jaroń, R. Hoffmann, A. Bergara, and N. W. Ashcroft, Phys. Rev. Lett. **96**, 017006 (2006).
[8] Y. Yao, J. S. Tse, Y. Ma and K. Tanaka, Europhys. Lett. **78**, 37003 (2007).
[9] M. I. Eremets, I. A. Trojan, S. A. Medvedev, J. S. Tse, Y. Yao, Science **319**, 1506 (2008).
[10] T. A. Strobel, A. F. Goncharov, C. T. Seagle, Z. Liu, M. Somayazulu, V. V. Struzhkin, and R. J. Hemley, Phys. Rev. B **83**, 144102 (2011).
[11] H. Wang, J. S. Tse, K. Tanaka, T. Iitaka, and Y. Ma, Proc. Nat. Acad. Sci. **109**, 6463 (2012).
[12] Y. Li, J. Hao, H. Liu, J. S. Tse, Y. Wang and Y. Ma, Sci. Rep. **5**, 9948 (2015).
[13] A. P. Drozdov, M. I. Eremets, I. A. Troyan, V. Ksenofontov, and S. I. Shylin, Nature **525**, 73 (2015).
[14] N. Bernstein, C. S. Hellberg, M. D. Johannes, I. I. Mazin, and M. J. Mehl, Phys. Rev. B **91**, 060511(R) (2015).
[15] D. Duan, X. Huang, F. Tian, D. Li, H. Yu, Y. Liu, Y. Ma, B. Liu, and T. Cui, Phys. Rev. B **91**, 180502(R) (2015).
[16] I. Errea, M. Calandra, C. J. Pickard, J. Nelson, R. J. Needs, Y. Li, H. Liu, Y. Zhang, Y. Ma, and F. Mauri, Phys. Rev. Lett. **114**, 157004 (2015).
[17] M. Einaga, M. Sakata, T. Ishikawa, K. Shimizu, M. I. Eremets, A. P. Drozdov, I. A. Troyan, N. Hirao and Y. Ohishi, Nat. Phys. **12**, 835 (2016).
[18] G. M. Eliashberg, Zh. Eksp. Teor. Fiz. **38**, 966 (1960) [Sov. Phys. JETP **11**, 696 (1960)].
[19] J. P. Carbotte, Rev. Mod. Phys. **62**, 1027 (1990).
[20] F. Marsiglio and J. P. Carbotte, in *Superconductivity: Conventional and Unconventional Superconductors* edited by K. H. Bennemann and J. B. Ketterson (Springer-Verlag, Berlin, 2008), p. 73.
[21] G. Bergmann and D. Rainer, Z. Phys. **263**, 59 (1973).
[22] B. Mitrovic and J. P. Carbotte, Solid State Commun. **40**, 249 (1981).
[23] Y. Yao, J. S. Tse, K. Tanaka, F. Marsiglio, and Y. Ma, Phys. Rev. B **79**, 054524 (2009).
[24] E. J. Nicol and J. P. Carbotte, Phys. Rev. B **91**, 220507(R) (2015).
[25] J. S. Tse, Y. Yao, and K. Tanaka, Phys. Rev. Lett. **98**, 117004 (2007).
[26] J. P. Carbotte, Sci. Prog. **71**, 329 (1987).
[27] Y. Wang, H. Wang, J. S. Tse, T. Iitaka and Y. Ma, Phys. Chem. Chem. Phys. **17**, 19379 (2015).
[28] W. L. McMillan, Phys. Rev. **167**, 331 (1968).
[29] P. B. Allen and R. C. Dynes, Phys. Rev. B **12**, 905 (1975).
[30] P. B. Allen and R. C. Dynes, J. Phys. C **8**, L158 (1975).
[31] P. Cudazzo, G. Profeta, A. Sanna, A. Floris, A. Continenza, S. Massidda, and E. K. U. Gross, Phys. Rev. Lett. **100**, 257001 (2008).

[32] H. Liu, I. I. Naumov, R. Hoffmann, N. W. Ashcroft, and R. J. Hemley, Proc. Nat. Acad. Sci. **114**, 6990 (2017).
[33] Our T_c values for YH_{10} and LaH_{10} are lower than those presented in Ref. 32 presumably due to different accuracies for solving the Eliashberg equations.